https://doi.org/10.5607/en23027
Exp Neurobiol. 2023 Dec;32(6):410-422.
pISSN 1226-2560 • eISSN 2093-8144

Original Article

Experimental Neurobiology

Peripheral Neuropathy and Decreased Locomotion of a *RAB40B* Mutation in Human and Model Animals

Wonseok Son[1†], Hui Su Jeong[2†], Da Eun Nam[1], Ah Jin Lee[1], Soo Hyun Nam[3], Ji Eun Lee[2,4*], Byung-Ok Choi[2,3,5*] and Ki Wha Chung[1*]

[1]Department of Biological Sciences and BK21 Team for Field-oriented BioCore Human Resources Development, Kongju National University, Gongju 32588, [2]Department of Health Sciences and Technology, Samsung Advanced Institute for Health Sciences & Technology, Sungkyunkwan University, Seoul 06351, [3]Cell and Gene Therapy Institute, Samsung Medical Center, Seoul 06351, [4]Samsung Biomedical Research Institute, Samsung Medical Center, Seoul 06351, [5]Department of Neurology, Samsung Medical Center, Sungkyunkwan University School of Medicine, Seoul 06351, Korea

Rab40 proteins are an atypical subgroup of Rab GTPases containing a unique suppressor of the cytokine signaling (SOCS) domain that is recruited to assemble the CRL5 E3 ligase complex for proteolytic regulation in various biological processes. A nonsense mutation deleting the C-terminal SOCS box in the *RAB40B* gene was identified in a family with axonal peripheral neuropathy (Charcot-Marie-Tooth disease type 2), and pathogenicity of the mutation was assessed in model organisms of zebrafish and *Drosophila*. Compared to control fish, zebrafish larvae transformed by the human mutant *hRAB40B-Y83X* showed a defective swimming pattern of stalling with restricted localization and slower motility. We were consistently able to observe reduced labeling of synaptic markers along neuromuscular junctions of the transformed larvae. In addition to the neurodevelopmental phenotypes, compared to normal *hRAB40B* expression, we further examined ectopic expression of *hRAB40B-Y83X* in *Drosophila* to show a progressive decline of locomotion ability. Decreased ability of locomotion by ubiquitous expression of the human mutation was reproduced not with GAL4 drivers for neuron-specific expression but only when a pan-glial GAL4 driver was applied. Using the ectopic expression model of *Drosophila*, we identified a genetic interaction in which *Cul5* down regulation exacerbated the defective motor performance, showing a consistent loss of SOCS box of the pathogenic RAB40B. Taken together, we could assess the possible gain-of-function of the human *RAB40B* mutation by comparing behavioral phenotypes in animal models; our results suggest that the mutant phenotypes may be associated with CRL5-mediated proteolytic regulation.

Key words: Peripheral neuropathy, *RAB40B*, SOCS box, Zebrafish, *Drosophila*

INTRODUCTION

The human genome comprises more than 60 Rab genes that make up one GTPase family; these genes have been studied mostly as molecular switches in intracellular membrane trafficking in various systems [1, 2]. Rab GTPases are key regulators also in animal nervous systems, exclusively in neurons across cell bodies to synapses; preferential subcellular localizations of each Rab protein are unique [3, 4]. Alterations of these Rab GTPases have been recognized to be associated with virtually all neuronal activities in health and disease. A well-known example is *RAB7A* mutations, which cause the neurodegenerative defects that are associated with

Submitted August 30, 2023, Revised December 13, 2023,
Accepted December 15, 2023

*To whom correspondence should be addressed.
Ji Eun Lee, TEL: 82-2-3410-6129, FAX: 82-2-3410-0534
e-mail: jieun.lee@skku.edu
Byung-Ok Choi, TEL: 82-2-3410-1296, FAX: 82-2-3410-0052
e-mail: bochoi77@hanmail.net
Ki Wha Chung, TEL: 82-41-850-8506, FAX: 82-41-850-0957
e-mail:kwchung@kongju.ac.kr
†These authors contributed equally to this article.

the autosomal dominant Charcot-Marie-Tooth disease type 2B (CMT2B) peripheral neuropathy [5-8]. CMT is the most common inherited peripheral neuropathy which is characterized by progressive distal muscle weakness and sensory impairment.

Rab40 proteins, consisting of four paralog members including RAB40B in humans, are an atypical subgroup of Rab proteins with unique structural and functional features. Besides the GTPase domain of the Rab family, Rab40 proteins are distinguished by an unusual domain of suppressor of cytokine signaling (SOCS) box in the C terminal part [9-11]. Group of proteins containing the SOCS box domain have typically been studied as adaptors that recruit substrates into a specific ubiquitination process of the Cullin-RING ligase 5 (CRL5) complex [12, 13]. A variety of SOCS box-containing substrate receptors are involved in each specific target degradation in various biological processes. Four important components of the E3 ligase complex are the CUL5 scaffold protein, elongin B/C, SOCS box-containing adaptors, and ring box protein 2 (RBX2) [12-14].

Among the four paralog members of human Rab40 proteins, RAB40B and RAB40C show preferentially higher expression in the nervous system and muscle tissues. However, little is known about the cellular functions of the Rab40 proteins beyond those structural features, except from studies on cellular adhesion and migration of several carcinoma cell lines. Both human RAB40A and RAB40C were shown to form complexes with CUL5 for proteasomal degradation of p21-activated kinase 4 (PAK4) and receptor for activated C kinase 1 (RACK1), respectively [10, 15]. Similarly, RAB40B-CUL5-dependent ubiquitination was found to regulate epithelial protein lost in neoplasm (EPLIN) localization and promote cell migration and invasion by altering focal adhesion and cytoskeletal dynamics in breast cancer cells [9, 16]. Other components of the CRL5 complex have also been linked to neuronal development, such as PAK4 kinase or RBX2-CUL5 complexes in proper axonal growth or neuronal migration [17, 18]. Thus, the overlapping tissue expression of Rab40s suggests a probability that those proteins may also be involved in neurodevelopmental and/or degenerative processes in the nervous system.

In the present study, we identified one *RAB40B* nonsense mutation from a CMT family that follows an autosomal dominant inheritance. Because there is no known evidence about neuronal functions of Rab40 proteins, we assessed the *in vivo* pathogenicity of the human mutation in the nervous system of model organisms, zebrafish and *Drosophila*. Based on the high sequence similarity and structural conservation between human and model animal Rab40 proteins, we examined the neuropathogenic effects of the *RAB40B* mutation using ectopic expression models.

MATERIALS AND METHODS

Participants

This study examined a Korean dominant CMT2 family with seven members including two affected individuals (family ID: FC162; Fig. 1A). Informed consent was obtained from all participants according to the protocol approved by the Institutional Review Board of Sungkyunkwan University, Samsung Medical Center (2014-08-057-002) and Kongju National University (KNU-IRB-2018-62).

Clinical assessment

Neuromuscular clinical phenotypes including motor and sensory impairments, deep tendon reflexes, and muscle atrophy were obtained in the standardized methods. Strengths of flexor and extensor muscles were assessed manually using the standard medical research council (MRC) scale [19]. To determine the severity of physical disability, we measured the functional disability scale (FDS), CMT neuropathy score version 2 (CMTNSv2), CMT examination score (CMTES), Rasch-modified CMTNSv2 (CMTNSv2-R), and Rasch-modified CMTES (CMTES-R) [20-23]. Sensory impairments were assessed in terms of the level and severity of pain, temperature, vibration, and position. Age at onset was determined by asking patients for their ages when symptoms, i.e., distal muscle weakness, foot deformity, or sensory change, first appeared.

Motor and sensory conduction velocities of median, ulnar, peroneal, and sural nerves were determined by standard methods using the surface stimulation and recording electrodes. Motor nerve conduction velocities (MNCVs) and compound muscle action potentials (CMAPs) of median nerves were determined by stimulating the elbow and wrist. In the same way, the MNCVs and CMAPs of peroneal nerves were determined by stimulating the knee and ankle. Amplitudes of CMAP were measured from baseline to negative peak values. Sensory nerve conduction velocities (SNCVs) were obtained over a finger-wrist segment from ulnar nerves and were also recorded for sural nerves. Sensory nerve action potential (SNAP) amplitudes were measured from positive peaks to negative peaks.

DNA extraction and genetic screening of the CMT family

Total DNA was extracted from blood obtained from participants using a HiGene Genomic DNA Prep Kit (Biofact, Daejeon, Korea). Exome capture and next generation sequencing were carried out using a SureSelect Human All Exon 50M kit (Agilent Technologies, Santa Clara, CA, USA) and HiSeq 2500 Genome Analyzers (Illumina, San Diego, CA, USA), respectively. Frequencies of

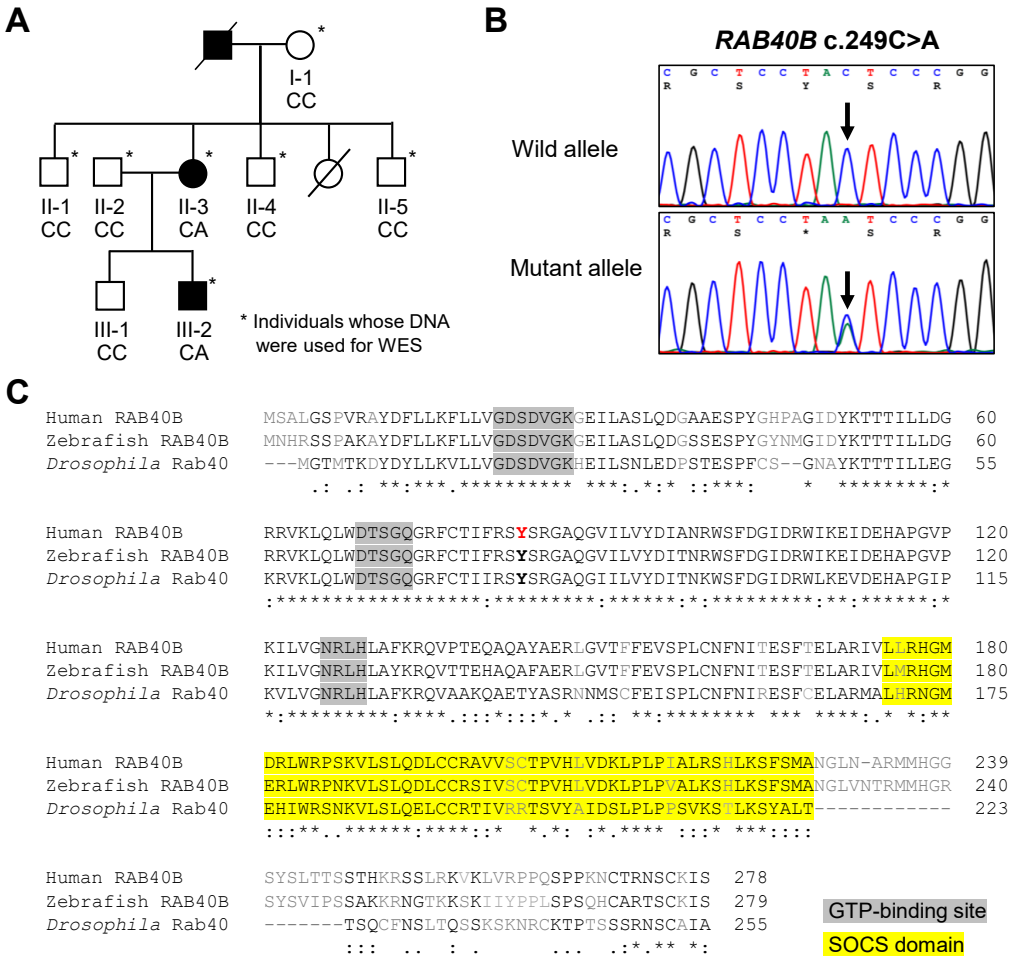

Fig. 1. Identification of *RAB40B* mutation in family with axonal neuropathic phenotype. (A) Pedigree of a CMT family (FC162) in which nonsense mutation of *RAB40B* was identified. Affected members are indicated by black boxes and circles. Genotypes of *RAB40B* c.249C>A are provided at the bottom of all the examined individuals. (B) Chromatograms of mutation sites. Black and red arrows indicate mutation site of rs781464100 (c.249C>A, p.Y83X). (C) Amino acid sequence alignment between human RAB40B and zebrafish and *Drosophila* homologs. The Rab40-characteristic SOCS domain is highlighted by yellow boxes. Position of the nonsense mutation (p.Y83X) is indicated by red letters.

rare alleles from the whole exome sequencing (WES) data were obtained from public human genome databases of the 1000 Genomes Project (http://www.1000genomes.org), the Genome Aggregation Database (https://gnomad.broadinstitute.org), and the Korean Reference Genome Database (http://coda.nih.go.kr/coda/KRGDB/index.jsp). Possible pathogenic variations were basically evaluated according to the American College of Medical Genetics and Genomics-Associations for Molecular Pathology (ACMG-AMP) guidelines (https://wintervar.wglab.org). Candidate pathogenic mutations found in the FC162 family were confirmed by Sanger sequencing of all participants.

Microinjection in zebrafish

Zebrafish (AB strain) were maintained with a cycle of 13-h light and 11-h dark in an automatic breeding system (Genomic-Design, Daejeon, Korea) at 28.5°C and pH 7.0~7.9, according to animal research protocols approved by the Institutional Animal Care and Use Committee of Samsung Biomedical Research Institute and Sungkyunkwan University (IACUC#20201008001 and IACUC#20200916001). The mutant *hRAB40B* ORF was subcloned into pCS2+ vector, and its capped mRNAs were synthesized using mMESSAGE mMACHINE SP6 kit (Ambion, Foster City, CA, USA). The *in vitro* synthesized *hRAB40B-Y83X* mRNAs (2,000 pg) were introduced into zebrafish embryos at the 1~2 cell stage using a gas-powered microinjection system (PV83 Pneumatic PicoPump, SYS-PV830; World Precision Instruments, Sarasota, FL, USA).

Zebrafish behavior analysis

Moving patterns and velocity of zebrafish larvae at 84 hours

 https://doi.org/10.5607/en23027

post-fertilization (hpf) were analyzed using DanioVision (Noldus, Wageningen, Netherlands). Behavioral analysis was performed using light stimulation in 1 ml zebrafish breeding media. Control zebrafish or *hRAB40B-Y83X* mRNA-injected zebrafish were placed in individual 24-well plates and their movements were recorded for 30 min and analyzed using EthoVision XT software (Noldus). All statistical analyses were performed using GraphPad Prism 5 (GraphPad, Boston, MA, USA). Values are presented as mean±SD or as fold change relative to the mean control. Differences between control and mRNA injected groups were evaluated using unpaired Student's t-test.

Immunohistochemistry of zebrafish tissues

Zebrafish larvae at 84 hpf were fixed in 4% paraformaldehyde in 0.1 M PBS overnight at 4°C. The larvae were permeabilized with 0.5% TritonX-100 in 0.1 M PBS (PBST) for 15 min at room temperature and washed with 1× PBS three times and blocked in 1% DMSO and 1% BSA in PBST containing 4% normal goat serum at room temperature for 1 hr. The following primary antibodies were used for incubation: mouse anti-SV2 (1:50; Developmental Studies Hybridoma Bank, Iowa City, IA, USA) and Alexa 647-conjugated α-BTX (B35450, 1:150; Invitrogen-ThermoFisher Scientific, Carlsbad, CA, USA) at 4°C overnight in blocking solution. After washing three times with PBST, larvae were treated with Alexa Fluor 488-conjugated secondary antibodies (A11001, 1:250; Life Technologies, Carlsbad, CA, USA) for 2 hr. at room temperature. The zebrafish larvae were mounted on slides with mounting solution containing n-propyl gallate and images were captured and analyzed with a confocal microscope (LSM 700; Carl Zeiss, Jena, Germany)/Zeiss ZEN imaging software and ImageJ (NIH, Bethesda, MD, USA). NMJs were analyzed by measuring the proportion of areas with merged yellow signals within the region of interest (ROI) of the zebrafish trunk.

Generation of transgenic flies

Human *RAB40B* cDNA (HG14600-G) was obtained from Sino Biological (Beijing, China). The p.Y83X mutation was introduced by site-directed PCR mutagenesis. *RAB40B* ORFs with or without the early stop codon were subcloned into pUAST-AttB transformation vector. Constructs were injected into *Drosophila* embryos for generation of transgenic strains (BestGene, Chino Hills, CA, USA). Genomic landing sites P40 and VK31 were used for site-directed transgene insertions on the second and third chromosome, respectively [24].

Drosophila strains

Rab40 and *Cul5* RNAi strains of the TRiP collection were obtained from Bloomington *Drosophila* Stock Center (BDSC; Bloomington, IN, USA). GAL4 strains were also sourced from BDSC, and used for ectopic expression described by followings: *Act5C-GAL4* [25] and *tub-GAL4* [26] for ubiquitous expression, *elav-GAL4* [27] and *nSyb-GAL4* [28] for pan-neuronal expression, *OK371* [29], *OK307* [30], and *D42-GAL4* [31] for expression in motor neurons, *ppk-GAL4* for expression in multidendritic neurons [32], and *repo-GAL4* for pan-glial expression [33]. Temperature-sensitive mutation of GAL80 repressor and its application for spatiotemporal gene expression were described by McGuire et al. [34]. Each GAL4 strain with the transgene of *tub-Gal80^{ts}* was crossed with *UAS-hRAB40B* flies at 20°C (permissive temperature), and newborn adults carrying all three transgenes were collected for temperature shift to the inducing temperature (30°C).

Drosophila locomotion analysis

Locomotion performance was measured by a climbing assay that uses the negative geotaxis behavior of flies [35]. Flies were collected daily for each genotype, put into groups of 10 to 15 individuals, and transferred to a 30°C chamber to induce transgene expression. Each group was assessed for climbing ability 2, 8, and 15 days after collection. Flies were put into test tubes of 18 cm length. After tapping tubes on a mouse pad to force out flies at the bottom, flies were allowed to climb the wall for one minute. Total numbers of flies that climbed over the marked height of 11 cm in the test tubes in three repeated tests were counted to calculate the climbing percentage. Four or six groups per genotype were assessed to calculate means and standard deviations.

RESULTS

Clinical manifestation in a CMT2 family with nonsense RAB40B mutation

In one CMT family (family ID: FC162), two individuals of mother and son were affected with axonal peripheral neuropathy (II-3 and III-2 in Fig. 1A). The clinical and electrophysiological features of the patients are shown in Table 1. Onset ages were 13 and 3 years old in mother and son, respectively. Muscle weakness and atrophy started and predominated in the distal portions of legs, and were noted to a lesser extent distally in upper limbs. Vibration sense was reduced to a greater extent than pain in the III-2 patient. Foot deformity and absent deep tendon reflex were shown in both patients, but scoliosis was found only in the mother (II-3). Functional disability was similar (FDS: 3), and CMTNSv2 was in the moderate category in both patients (17 and 13, respectively). However, when considering the disease duration, the son was more

Table 1. Clinical and electrophysiological features in CMT2 patients of FC162 family

Phenotypes/patients (sex)	II-3 (female)	III-2 (male)
Age at onset/examination (years)	13/42	3/8
Muscle weakness in limb (upper/lower)[a]	++/+++	+/+++
Muscle atrophy	Moderate	Mild
Foot deformities	Yes	Yes
Pinprick sense in limb (upper/lower)	Reduced/reduced	Mildly reduced/reduced
Vibration in limb (upper/lower)	Reduced/reduced	Mildly reduced/reduced
Deep tendon reflex (knee and ankle jerk)	Absent	Absent
Scoliosis	Yes	Yes
Pyramidal sign	No	No
Brainstem auditory evoked potential	Not done	Normal
FDS	3 (walking difficulty)	3 (walking difficulty)
CMTNSv2/CMTNSv2-R	17 (moderate)/22 (severe)	13 (moderate)/18 (moderate)
CMTES/CMTES-R	15 (severe)/19 (severe)	12 (moderate)/16 (moderate)
Motor nerve conduction[b]		
Median CMAP (mV)/MNCV (m/s)	13.5/42.5	11.8/46.3
Peroneal CMAP (mV)/MNCV (m/s)	Absent/absent	Absent/absent
Sensory nerve conduction[b]		
Ulnar SNAP (μV)/SNCV (m/s)	7.2/28.2	12.9/29.8
Sural SNAP (μV)/SNCV (m/s)	Absent/absent	Absent/absent

CMAP, compound muscle action potential; CMTES, CMT examination score; CMTES-R, Rasch-modified CMTES; CMTNSv2, CMT neuropathy score version 2; CMTNSv2-R, Rasch-modified CMTNSv2; FDS, functional disability scale; MNCV, motor nerve conduction velocity; SNAP, sensory nerve action potential; SNCV, sensory nerve conduction velocity.

[a]Upper limb: + and ++ = intrinsic hand weakness 4/5 and < 4/5 on the MRC scale. Lower limb: + and ++ = ankle dorsiflexion 4/5 and < 4/5 on the MRC scale; +++ = proximal weakness.

[b]Normal voltages of motor median nerve ≥6 mV, peroneal nerve ≥1.6 mV, sensory ulnar nerve ≥7.9 μV, and sural nerve ≥6.0 μV; normal conduction velocities of motor median nerve ≥50.5 m/s, peroneal nerve ≥41.2 m/s, sensory ulnar nerve ≥37.5 m/s and sural nerve ≥32.1 m/s.

severely affected than his mother. Motor and sensory conduction studies were carried out in both patients (Table 1). Electrophysiological findings confirmed that both patients were axonal type of CMT2 neuropathy.

In the mutation screen by WES for the FC162 family, we identified a nonsense mutation in the *RAB40B* gene (rs781464100, c.249C>A, p.Y83X, Fig. 1B) specific to the affected members. The early stop codon of the deduced sequences is expected to generate a truncated product that lacks its C-terminal SOCS box domain of the atypical Rab protein (Fig. 1C). Although no other candidate mutation was identified in the exome sequencing for the familial neuropathic phenotype, more evidences are required to evaluate the pathogenicity of the *RAB40B* mutation.

In sequence comparison of human RAB40B to zebrafish and *Drosophila* homologs, high sequence similarity was confirmed along the GTPase domain and the SOCS box sequences, as well as around the nonsense mutation site (Fig. 1C). Based on the sequence and structural homology between humans and the model animal Rab40 proteins, we examined the *in vivo* pathogenicity of the human mutation using zebrafish and *Drosophila* platforms.

Transient transformation with human RAB40B-Y83X induced motility defects in zebrafish

The *RAB40B* mutation in the FC162 family with the neuropathic phenotypes were manifested with the nonsense mutation, which followed an autosomal dominant inheritance (Fig. 1A). Based on the inheritance pattern and the presumptive pathogenic cause of the *RAB40B* mutation, we examined ectopic expression phenotypes of the human mutation in model organisms of zebrafish and *Drosophila*.

Capped mRNAs of human *RAB40B* with the early stop mutation were prepared *in vitro* and introduced into zebrafish embryos for transformation with the probable pathogenic sequences. Using the ectopic expression model of zebrafish, we observed that exogenous human mutant *hRAB40B* led to nonsignificant developmental delay (Fig. 2A). But when we investigated the effect of human mutation on motility by testing the transformant's swimming pattern. We noticed that 84 hpf-larvae transformed by the mutant *hRAB40B* stalled with restricted localization, whereas control zebrafish swam throughout the tested area (Fig. 2B). The zebrafish locomotion velocity was measured, and we found that the *hRAB40B-Y83X* transformants moved more slowly than control and Mock-expressing fish (Fig. 2C).

Based on the larval motility defect, we examined neurodevelopmental phenotypes induced by the *hRAB40B-Y83X* transformation in formation of neuromuscular junctions (NMJs). In zebrafish, SV2 (synaptic vesicle protein 2) staining reveals synaptic vesicles in motor axons and terminals; thus, staining has been

https://doi.org/10.5607/en23027

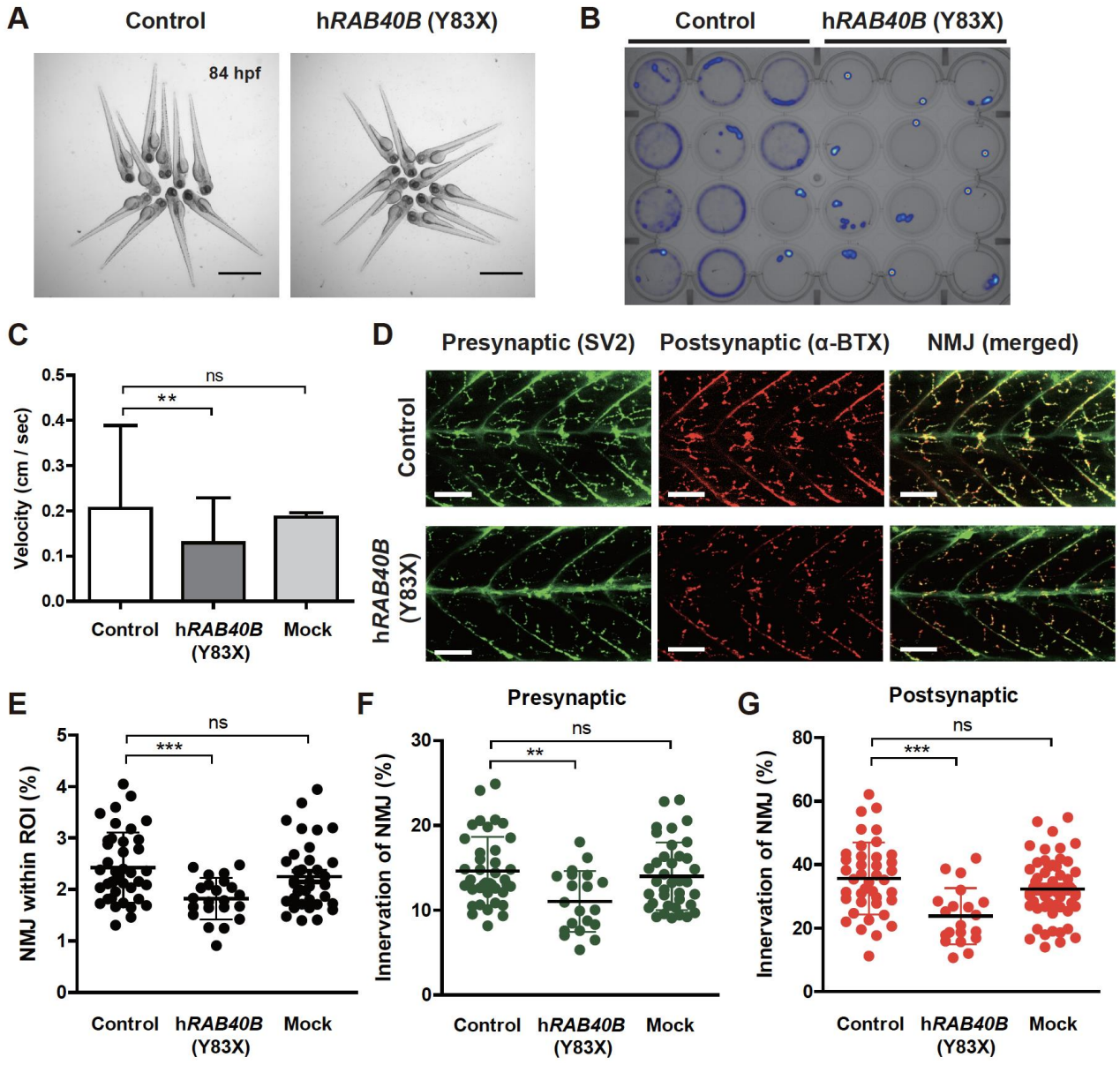

Fig. 2. Zebrafish transformed by mutant *hRAB40B* showed motility defects. (A) Developmental morphologies of control, Mock or exogenous *hRAB40B-Y83X* mRNA-expressed larvae at 84 hpf. Scale bars, 2,000 μm. (B) Heatmap images showing swimming patterns between the control and *hRAB40B-Y83X* mRNA-injected zebrafish larvae. (C) Quantification of velocity analyzed in control zebrafish (n=65), Mock-expressing zebrafish (n=70), and *hRAB40B-Y83X*-transformant zebrafish (n=76). (D) Lateral view images after staining with α-SV2 (presynaptic region) and α-BTX (postsynaptic region) of the whole-mounted zebrafish at 84 hpf. Scale bars, 50 μm. (E) Comparison of NMJ signal ratios within ROI among control (n=43), Mock-expressing zebrafish (n=20), and *hRAB40B-Y83X*-transformant zebrafish (n=22). Comparisons of NMJ innervation in the presynaptic area (F) and postsynaptic area (G) among control (n=40), Mock-expressing zebrafish (n=23) and *hRAB40B-Y83X*-transformant zebrafish (n=20). Statistical significance was determined using an unpaired Student's t-test (**p<0.01, ***p<0.001).

used to label the presynaptic terminals of NMJ. Neuromuscular synapses can be visualized when presynaptic SV2-stained vesicle clusters (green in Fig. 2D) are opposed to postsynaptic α-BTX (bungarotoxin)-stained AChR clusters (red in Fig. 2D) [36, 37]. We found that *hRAB40B-Y83X*-transformant zebrafish were labeled less often by both pre- and postsynaptic markers in the larval NMJs (Fig. 2D, E). In addition, we analyzed the extent of NMJ innervation in the NMJ areas of *hRAB40B-Y83X* larvae (Fig. 2F, G) with those of control or Mock-expressing larvae. The zebrafish expressing *hRAB40B-Y83X* had less innervation signals than the control and Mock-expressing fish in both presynaptic and postsynaptic regions of the NMJ (Fig. 2F, G). This neurodevelopmental

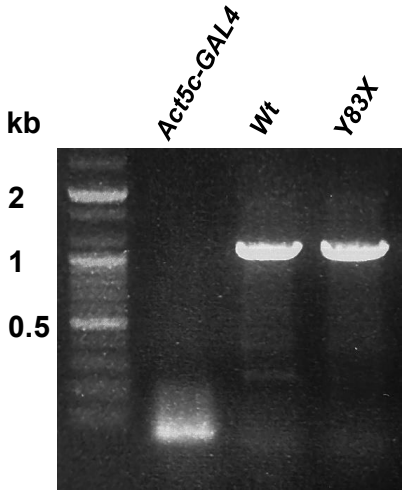

Fig. 3. Expressions of the *hRAB40B* in the transgenic embryos. After establishment of *hRAB40B* transgenic strains, expressions of the transformed genes were confirmed by RT-PCR in embryos from crosses of the transgenic flies with GAL4 drivers. *Act5c-GAL4* is used for the control (Wt: *Act5c>hRAB40B-wt*, *Y83X*: *Act5c>hRAB40B-Y83X*).

phenotype in NMJ formation is consistent with motility defects induced by transformation with the human mutant sequences, suggesting a possible neuropathic causality of the *RAB40B* mutation.

Ectopic expression of hRAB40B-Y83X reproduced defective motor performance in Drosophila

A stable transgenic model of the human *RAB40B* mutation was established in *Drosophila* to examine neuropathic impairments by mutant sequences beyond developmental phenotypes. Expression of the *hRAB40B* in the transgenic embryos were confirmed by RT-PCR (Fig. 3) Transgenic strains of the human *RAB40B* gene or its nonsense mutant form were prepared by site-directed integration of corresponding transgenes [24]. First, ectopic expression of those human genes, as well as RNAi knockdown of *Drosophila Rab40*, were examined for developmental effects by ubiquitous expression driven by *Act5c-GAL4*.

Semi-lethality was shown by ubiquitous expressions of both the wild and mutant *hRAB40B* (18.1% and 27.1% failure during the larval and pupal development of *Act>hRAB40B* (n=199) and *Act>hRAB40B-Y83X* (n=236), respectively); however, majority of the ectopic expression progeny succeeded in development to adults. The adult survivors showed no detectable morphological defects, except reduced lifespans (half survival rate around 20 days after hatching). In addition, delayed larval development was shown by expression of both forms of human *RAB40B*, as well as by RNAi knockdown of the *Drosophila* homolog (from two- to four days-delay on average, depending on culture vials). As for the downregulation of *Drosophila Rab40*, we established a balanced stock that expressed its dsRNAs ubiquitously and constantly. Except for delayed development for few days as well, the interim stock showed no detectable phenotype for generations, suggesting that the *Drosophila Rab40* by itself is near a dispensable gene for normal development.

Parallel to the motility test of zebrafish transformants, we examined the larval locomotive abilities of the progeny of ectopic expressions of *hRAB40B* genes or *Rab40* RNAi knockdown in *Drosophila*. Due to the delayed larval growth depending on genotypes, the early third instar larvae for the locomotion test were collected based on body size from groups of different culture days. However, it was hard to find any distinguishable difference in larval crawling ability among different genetic conditions of *hRAB40B* or *Drosophila Rab40*, including expression of human mutation (data not shown).

Then, in adult animals, we tested the dominant pathogenicity of the human mutation to find similar degenerative hallmarks by its ectopic expression in *Drosophila*. To avoid any developmental effects of *hRAB40B* expression, we applied a temporal expression system using a temperature-sensitive mutation of GAL80 (*tub-Gal80^{ts}*) for ectopic expression of the transgenes [34]. Under the *tub-Gal80^{ts}* system, locomotion abilities of flies expressing *hRAB40B* at the inducing temperature after hatching were examined to recapitulate neuropathic phenotypes of the human mutation. The locomotion ability was assessed quantitatively by a climbing assay. First, the human *RAB40B* was expressed ubiquitously by *tub-GAL4*. When comparing motor abilities after expression of the wild and mutant *hRAB40B*, we were able to discern a difference between those ectopic expressions, with a progressive decline of motor performance when mutant *hRAB40B* was expressed (Fig. 4A, 4B, *tub-GAL4*). Further, we examined the constant expression of *Rab40* dsRNAs on the motor performance by adult ages. Differently from temporal expression of the human mutation, the constant downregulation of the *Drosophila* homolog itself did not show a locomotive decline by ages (data not shown), suggesting that the defective motor performance by the mutant *hRAB40B* is a gain-of-function phenotype of the mutation rather than a loss-of-function condition of *Rab40*.

Next, we sought to determine whether the progressive motor defect was of neuron-origin. Several specific GAL4 drivers were introduced for ectopic expression in the nervous system, such as pan-neuronal GAL4s, *elav-GAL4* and *nSyb-GAL4*, and neuron type-specific GAL4s like *OK371* or *OK307* for expression in motor neurons [29, 30], *ppk-GAL4* for expression in sensory neurons [32], and *D42-GAL4* for expression in synapses with the musculature [31]. However, we failed to find a GAL4 driver among those

https://doi.org/10.5607/en23027

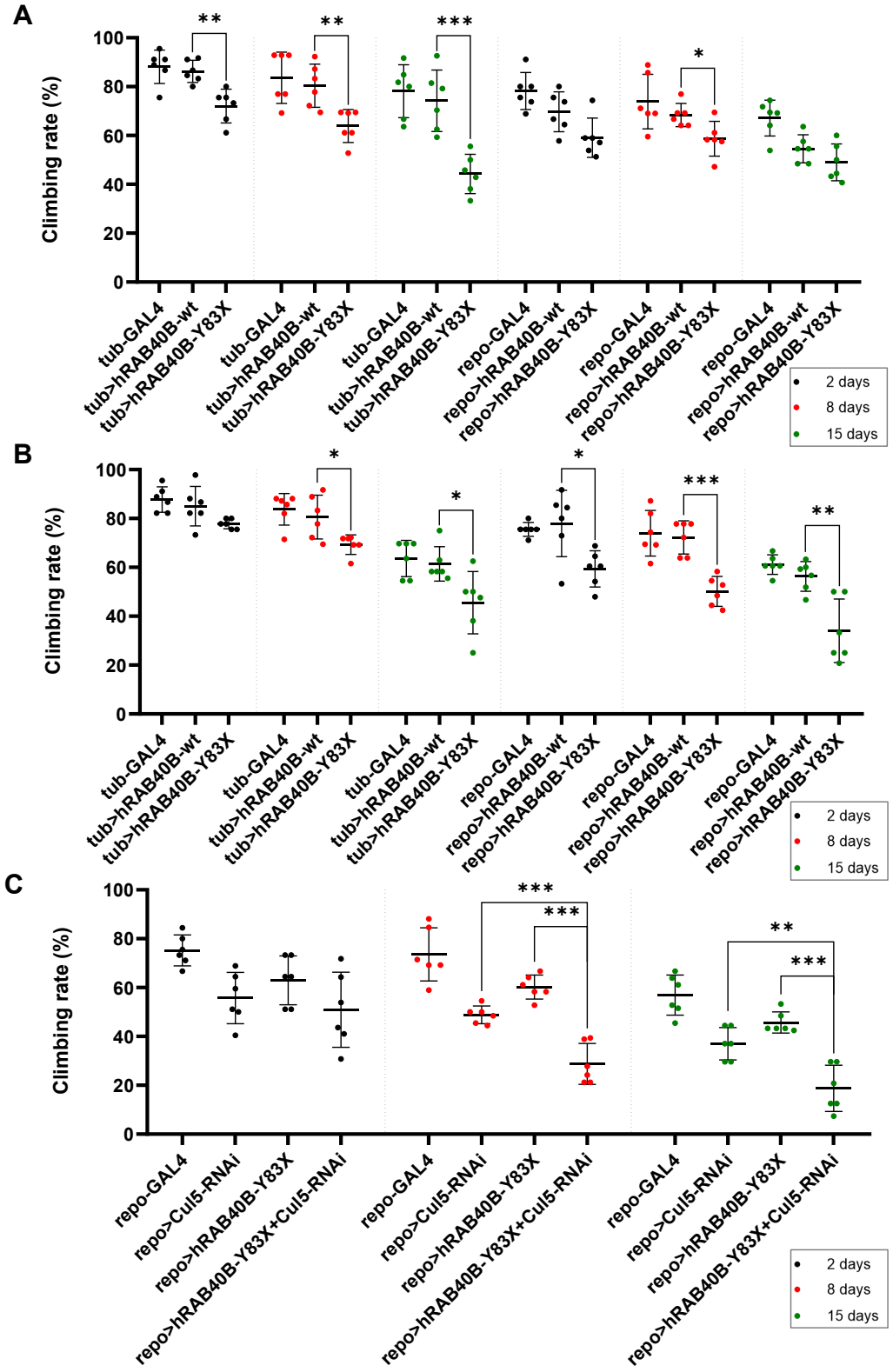

Fig. 4. Reduced locomotion ability by ectopic expression of the C-terminal truncation mutation of *hRAB40B*. The locomotion ability of adult flies was quantified in a climbing assay. Progressive deterioration of motor performance was shown when the mutant *hRAB40B* was expressed ubiquitously (A, B, *tub-GAL4*) or under control of the pan-glial *repo-GAL4* (B), but not with *OK371* (A) or other neuron-specific GAL4 drivers. (C) The *Drosophila Cul5* knockdown enhanced the locomotion defect with expression of the mutant *hRAB40B*, showing a genetic interaction of the defective motor phenotype with the CRL5-mediated proteolytic regulation (tested groups of each genotype, n=6; *p<0.05, **p<0.01, ***p<0.001).

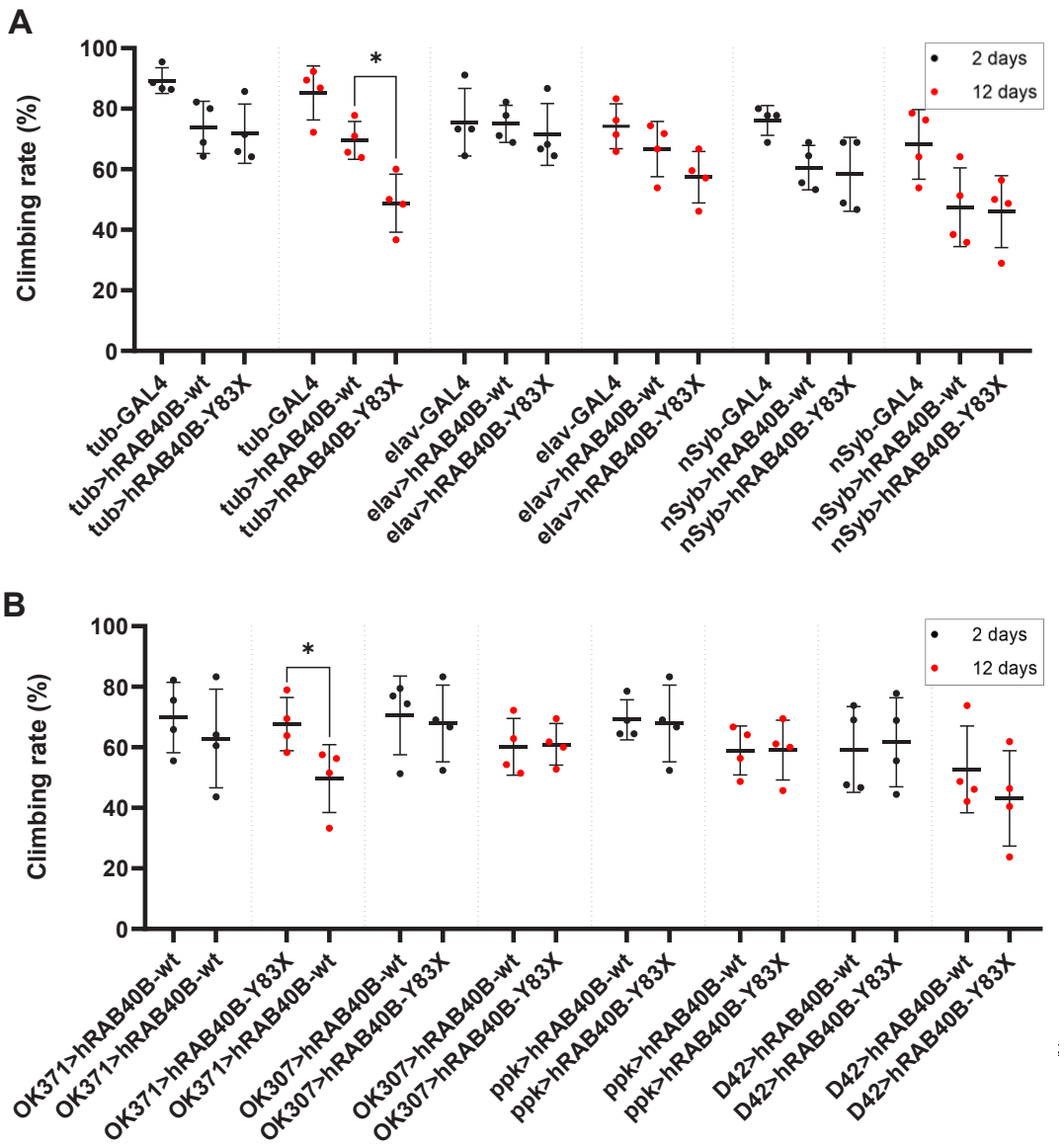

Fig. 5. Locomotion abilities after ectopic expression of the mutant *hRAB40B* under control of *tub-GAL4* or neuron-specific GAL4 drivers. The locomotion ability of adult flies was quantified in a climbing assay. A ubiquitous expression of the mutant *hRAB40B* reduced climbing ability (A, *tub-GAL4*). Repetition of the defective motor phenotype was assessed with neuron-specific GAL4 drivers: (A) *elav-GAL4* or *nSyb-GAL4* and (B) *OK371*, or *OK307*, *ppk-GAL4*, *D42-GAL4* (tested groups of each genotype, n=4; *p<0.05).

that could reproduce the locomotion defect shown by ubiquitous expression of the mutant *hRAB40B* (Fig. 4A, 5).

We also tested expression in glial cells, the other cell type in the nervous system. A similar behavioral defect was found when the pan-glial GAL4, *repo-GAL4* [33] was applied for the mutant *hRAB40B* expression (Fig. 4B). Ectopic expression driven by *repo-GAL4* exactly repeated the progressive decline of motor performance shown by ubiquitous expression of the human mutation. Thus, the deteriorating locomotion ability of the mutant *hRAB40B* was not caused by its neuronal expression, but was reproduced under control of the pan-glial GAL4, suggesting an association of the *Drosophila* glial system with the behavioral phenotype.

Cul5 downregulation enhanced defective motor phenotype of mutant hRAB40B expression

The unique SOCS box domain of Rab40 proteins induces physical interactions with CUL5 and other essential components of the CRL5 complex to target specific substrates of the ubiquitination system [12, 13]. The pleiotropic developmental functions of *Drosophila Cul5* have been reported predominantly in the female

https://doi.org/10.5607/en23027

germ line, as well as in larval neuromuscular junctions [38, 39]. To examine the prepotent molecular pathway underlying the defective motor performance caused by the C-terminally truncated human RAB40B, we tested *Cul5* knockdown to modify the mutant *hRAB40B*-induced motor phenotypes.

Since ubiquitous downregulation of *Cul5* led to a partial developmental failure (data not shown), epistatic effects of the *Cul5* knockdown were also assessed in the *tub-Gal80^{ts}* system. Under control of the pan-glial *repo-GAL4*, downregulation of *Drosophila Cul5* was found to synergistically enhance the defective motor phenotype of the mutant *hRAB40B* (Fig. 4C). Though a direct physical interaction should be identified between the human product and the *Drosophila* ubiquitination unit, this genetic interaction result suggests a possibility that the locomotion defect caused by the human mutation may be associated with the CRL5-dependent proteolytic regulation that is conserved between *Drosophila* and vertebrates.

DISCUSSION

In this study using ectopic expression models of zebrafish and *Drosophila*, we assessed *in vivo* effects of a *RAB40B* mutation observed in a family with autosomal dominant axonal neuropathies. By introduction of the human mutation, we were able to identify behavioral phenotypes similar to human neuropathic symptoms such as a motility defect of zebrafish larvae and a progressive decline of locomotion ability in *Drosophila*. This is the first evidence that an alteration of Rab40 proteins is associated with clinical phenotypes, which is consistent with preferential expression of the atypical Rab protein in the human nervous system.

Despite the successful establishment of animal models for the *RAB40B* nonsense mutation, there are presently many model limitations when analyzing human neuropathic symptoms. Distinct neurodevelopmental phenotypes were manifested in the transformed zebrafish, such as defective larval motility and reduced synaptic marks in NMJs (Fig. 2); however, in the *Drosophila* transgenic model, a probable defect in larval crawling ability was below the detection limit, despite a portion of the developmental failure being due to *hRAB40B* expression. Instead, in adult flies, we were able to reproduce an ectopic expression-induced progressive deterioration of locomotion ability (Fig. 4). Moreover, despite the phenotypic similarity of the ectopic expressional traits to the human neuropathic symptoms, we do presently not have enough evidence of the molecular pathways underlying the pathogenic phenotypes by the *RAB40B* mutation, except for genetic interaction with the *Cul5* knockdown in the *Drosophila* model. For this reason, strict evaluation of our established models will require further work, such as screening of target substrates that are regulated by the probable RAB40B-involved proteolytic regulation.

In the present study, we utilized zebrafish transformants and *Drosophila* transgenic animals. The human genome comprises four paralogs of Rab40s, and zebrafish and *Drosophila* retain only two and a homolog of Rab40 genes, respectively. Because these paralogs are possibly involved in different biological processes despite those high homologies, the zebrafish system may be suitable for detailed analysis of human mutation. It will thus be promising in future to develop transgenic models of zebrafish or other mammalian organisms.

Rab40 proteins, including human RAB40B, share a unique C-terminal SOCS box domain, which is a key motif to assemble the CRL5 ubiquitin ligase complex [12, 13]. Thus, mutations across the binding motif may cause a dominant-negative result against proteolytic regulation of specific targets of the Rab40 adaptors [9, 10]. In this study, we identified a genetic interaction between ectopic expression of the SOCS box-deficient *hRAB40B* and *Drosophila Cul5* knockdown that enhances locomotion defects (Fig. 4C). When considering neurodevelopmental and degenerative phenotypes caused by alterations of human and *Drosophila* CUL5s [17, 18, 38, 40], this result supports functional conservation of the specific proteolytic regulation in the nervous system from *Drosophila* to human, and suggests that the dominant locomotive defects induced by the SOCS box-lacking *RAB40B* mutation may be associated with the conserved process of CRL5 ubiquitination. Though the direct interaction of the human product with *Drosophila* CRL5 complex remains to be clarified, the epistatic behavioral modification may be a significant clue to trace the molecular pathogenesis of the human mutation.

In the *Drosophila* model, the defective motor performance induced by the *hRAB40B* mutation was displayed not by neuronal GAL4 drivers, but was reproduced under control of the pan-glial *repo-GAL4*. The glial systems of *Drosophila* and vertebrates share crucial cellular functions of metabolic sustenance and immune support, and in regulation of synaptic plasticity [41-43]. However, the *Drosophila* glia comprises only limited cell numbers in adult CNS when compared to mammalians, further, *Drosophila* lacks myelin sheaths and Schwan cells that are exclusively developed in the vertebrate nervous system. Due to these reasons, *Drosophila* models for neuropathic phenotypes have been established mostly for the axonal type CMT, whereas demyelinating disorders are a representative pathogenesis for human peripheral neuropathies. However, a mitochondrial disorder in a group of glial cells was recently reported to induce progressive locomotion defect in *Drosophila* [44]. Like the SOCX mutants, a group of neuropathic phenotypes may be caused from glial defects but independent on

demyelination. Besides developmental roles of glial cells in organization of the nervous system, little is known about glial functions for degenerating phenotypes in the adult nervous system. Though more evidence for molecular pathogenesis of the *hRAB40B* mutation should be elucidated to address glial causality of the mutation, the present study may provide a novel example of neuropathic phenotypes caused by an alteration in the glial system.

Taken together, our results so far evidence a probable pathogenic gain-of-function of the *RAB40B* mutation lacking the C-terminal SOCS box, and show that ectopic expressional locomotive defects in model animals may be associated with an alteration of the CRL5 complex-mediated proteolytic regulation in the glial system. Nevertheless, it seems that further studies are necessary to solve the controversies between the locomotion defect in the flies of pan-glial expression of the *hRAB40B* mutation and the axonal defective CMT phenotype in the examined family.

ACKNOWLEDGEMENTS

This study was supported by the National Research Foundation of Korea (2021R1A4A2001389, 2021R1A6A3A123041249, 2021R1A2C3004572, and 2022R1I1A2068995), Korean Health Technology R&D Project, Ministry of Health and Welfare (HR22C1363), and Future Medicine 2030 Project of the Samsung Medical Center (SMX122005).

REFERENCES

1. Li G, Marlin MC (2015) Rab family of GTPases. Methods Mol Biol 1298:1-15.
2. Stenmark H (2009) Rab GTPases as coordinators of vesicle traffic. Nat Rev Mol Cell Biol 10:513-525.
3. Kiral FR, Kohrs FE, Jin EJ, Hiesinger PR (2018) Rab GTPases and membrane trafficking in neurodegeneration. Curr Biol 28:R471-R486.
4. Dunst S, Kazimiers T, von Zadow F, Jambor H, Sagner A, Brankatschk B, Mahmoud A, Spannl S, Tomancak P, Eaton S, Brankatschk M (2015) Endogenously tagged rab proteins: a resource to study membrane trafficking in Drosophila. Dev Cell 33:351-365.
5. BasuRay S, Mukherjee S, Romero E, Wilson MC, Wandinger-Ness A (2010) Rab7 mutants associated with Charcot-Marie-Tooth disease exhibit enhanced NGF-stimulated signaling. PLoS One 5:e15351.
6. BasuRay S, Mukherjee S, Romero EG, Seaman MN, Wandinger-Ness A (2013) Rab7 mutants associated with Charcot-Marie-Tooth disease cause delayed growth factor receptor transport and altered endosomal and nuclear signaling. J Biol Chem 288:1135-1149.
7. Cherry S, Jin EJ, Ozel MN, Lu Z, Agi E, Wang D, Jung WH, Epstein D, Meinertzhagen IA, Chan CC, Hiesinger PR (2013) Charcot-Marie-Tooth 2B mutations in rab7 cause dosage-dependent neurodegeneration due to partial loss of function. Elife 2:e01064.
8. Spinosa MR, Progida C, De Luca A, Colucci AM, Alifano P, Bucci C (2008) Functional characterization of Rab7 mutant proteins associated with Charcot-Marie-Tooth type 2B disease. J Neurosci 28:1640-1648.
9. Linklater ES, Duncan ED, Han KJ, Kaupinis A, Valius M, Lyons TR, Prekeris R (2021) Rab40-Cullin5 complex regulates EPLIN and actin cytoskeleton dynamics during cell migration. J Cell Biol 220:e202008060.
10. Day JP, Whiteley E, Freeley M, Long A, Malacrida B, Kiely P, Baillie GS (2018) RAB40C regulates RACK1 stability via the ubiquitin-proteasome system. Future Sci OA 4:FSO317.
11. Tan R, Wang W, Wang S, Wang Z, Sun L, He W, Fan R, Zhou Y, Xu X, Hong W, Wang T (2013) Small GTPase Rab40c associates with lipid droplets and modulates the biogenesis of lipid droplets. PLoS One 8:e63213.
12. Okumura F, Joo-Okumura A, Nakatsukasa K, Kamura T (2016) The role of cullin 5-containing ubiquitin ligases. Cell Div 11:1.
13. Zhao Y, Xiong X, Sun Y (2020) Cullin-RING ligase 5: functional characterization and its role in human cancers. Semin Cancer Biol 67(Pt 2):61-79.
14. Hilton DJ, Richardson RT, Alexander WS, Viney EM, Willson TA, Sprigg NS, Starr R, Nicholson SE, Metcalf D, Nicola NA (1998) Twenty proteins containing a C-terminal SOCS box form five structural classes. Proc Natl Acad Sci U S A 95:114-119.
15. Dart AE, Box GM, Court W, Gale ME, Brown JP, Pinder SE, Eccles SA, Wells CM (2015) PAK4 promotes kinase-independent stabilization of RhoU to modulate cell adhesion. J Cell Biol 211:863-879.
16. Shi LW, Zhao ZB, Zhong L, Gao J, Gong JP, Chen H, Min Y, Zhang YY, Li Z (2020) Overexpression of Rab40b promotes hepatocellular carcinoma cell proliferation and metastasis via PI3K/AKT signaling pathway. Cancer Manag Res 12:10139-10150.
17. Qu J, Li X, Novitch BG, Zheng Y, Kohn M, Xie JM, Kozinn S, Bronson R, Beg AA, Minden A (2003) PAK4 kinase is essential for embryonic viability and for proper neuronal development. Mol Cell Biol 23:7122-7133.
18. Simó S, Cooper JA (2013) Rbx2 regulates neuronal migration

through different cullin 5-RING ligase adaptors. Dev Cell 27:399-411.
19. Paternostro-Sluga T, Grim-Stieger M, Posch M, Schuhfried O, Vacariu G, Mittermaier C, Bittner C, Fialka-Moser V (2008) Reliability and validity of the Medical Research Council (MRC) scale and a modified scale for testing muscle strength in patients with radial palsy. J Rehabil Med 40:665-671.
20. Birouk N, Gouider R, Le Guern E, Gugenheim M, Tardieu S, Maisonobe T, Le Forestier N, Agid Y, Brice A, Bouche P (1997) Charcot-Marie-Tooth disease type 1A with 17p11.2 duplication. Clinical and electrophysiological phenotype study and factors influencing disease severity in 119 cases. Brain 120(Pt 5):813-823.
21. Murphy SM, Herrmann DN, McDermott MP, Scherer SS, Shy ME, Reilly MM, Pareyson D (2011) Reliability of the CMT neuropathy score (second version) in Charcot-Marie-Tooth disease. J Peripher Nerv Syst 16:191-198.
22. Sadjadi R, Reilly MM, Shy ME, Pareyson D, Laura M, Murphy S, Feely SM, Grider T, Bacon C, Piscosquito G, Calabrese D, Burns TM (2014) Psychometrics evaluation of Charcot-Marie-Tooth Neuropathy Score (CMTNSv2) second version, using Rasch analysis. J Peripher Nerv Syst 19:192-196.
23. Micallef J, Attarian S, Dubourg O, Gonnaud PM, Hogrel JY, Stojkovic T, Bernard R, Jouve E, Pitel S, Vacherot F, Remec JF, Jomir L, Azabou E, Al-Moussawi M, Lefebvre MN, Attolini L, Yaici S, Tanesse D, Fontes M, Pouget J, Blin O (2009) Effect of ascorbic acid in patients with Charcot-Marie-Tooth disease type 1A: a multicentre, randomised, double-blind, placebo-controlled trial. Lancet Neurol 8:1103-1110.
24. Bischof J, Maeda RK, Hediger M, Karch F, Basler K (2007) An optimized transgenesis system for Drosophila using germ-line-specific phiC31 integrases. Proc Natl Acad Sci U S A 104:3312-3317.
25. Ito K, Awano W, Suzuki K, Hiromi Y, Yamamoto D (1997) The Drosophila mushroom body is a quadruple structure of clonal units each of which contains a virtually identical set of neurones and glial cells. Development 124:761-771.
26. Lee T, Luo L (1999) Mosaic analysis with a repressible cell marker for studies of gene function in neuronal morphogenesis. Neuron 22:451-461.
27. Lin DM, Goodman CS (1994) Ectopic and increased expression of Fasciclin II alters motoneuron growth cone guidance. Neuron 13:507-523.
28. Pauli A, Althoff F, Oliveira RA, Heidmann S, Schuldiner O, Lehner CF, Dickson BJ, Nasmyth K (2008) Cell-type-specific TEV protease cleavage reveals cohesin functions in Drosophila neurons. Dev Cell 14:239-251.
29. Kolodziejczyk A, Sun X, Meinertzhagen IA, Nässel DR (2008) Glutamate, GABA and acetylcholine signaling components in the lamina of the Drosophila visual system. PLoS One 3:e2110.
30. Allen MJ, Drummond JA, Moffat KG (1998) Development of the giant fiber neuron of Drosophila melanogaster. J Comp Neurol 397:519-531.
31. Sanyal S (2009) Genomic mapping and expression patterns of C380, OK6 and D42 enhancer trap lines in the larval nervous system of Drosophila. Gene Expr Patterns 9:371-380.
32. Grueber WB, Ye B, Yang CH, Younger S, Borden K, Jan LY, Jan YN (2007) Projections of Drosophila multidendritic neurons in the central nervous system: links with peripheral dendrite morphology. Development 134:55-64.
33. Awasaki T, Ito K (2004) Engulfing action of glial cells is required for programmed axon pruning during Drosophila metamorphosis. Curr Biol 14:668-677.
34. McGuire SE, Roman G, Davis RL (2004) Gene expression systems in Drosophila: a synthesis of time and space. Trends Genet 20:384-391.
35. Madabattula ST, Strautman JC, Bysice AM, O'Sullivan JA, Androschuk A, Rosenfelt C, Doucet K, Rouleau G, Bolduc F (2015) Quantitative analysis of climbing defects in a Drosophila model of neurodegenerative disorders. J Vis Exp 100:e52741.
36. Panzer JA, Gibbs SM, Dosch R, Wagner D, Mullins MC, Granato M, Balice-Gordon RJ (2005) Neuromuscular synaptogenesis in wild-type and mutant zebrafish. Dev Biol 285:340-357.
37. Jeong HS, Kim HJ, Kim DH, Chung KW, Choi BO, Lee JE (2022) Therapeutic potential of CKD-504, a novel selective histone deacetylase 6 inhibitor, in a zebrafish model of neuromuscular junction disorders. Mol Cells 45:231-242.
38. Ayyub C (2011) Cullin-5 and cullin-2 play a role in the development of neuromuscular junction and the female germ line of Drosophila. J Genet 90:239-249.
39. Ayyub C, Sen A, Gonsalves F, Badrinath K, Bhandari P, Shashidhara LS, Krishna S, Rodrigues V (2005) Cullin-5 plays multiple roles in cell fate specification and synapse formation during Drosophila development. Dev Dyn 232:865-875.
40. Reynolds PJ, Simms JR, Duronio RJ (2008) Identifying determinants of cullin binding specificity among the three functionally different Drosophila melanogaster Roc proteins via domain swapping. PLoS One 3:e2918.
41. Edwards TN, Meinertzhagen IA (2010) The functional organisation of glia in the adult brain of Drosophila and other insects. Prog Neurobiol 90:471-497.

42. Kremer MC, Jung C, Batelli S, Rubin GM, Gaul U (2017) The glia of the adult Drosophila nervous system. Glia 65:606-638.
43. Kim T, Song B, Lee IS (2020) Drosophila glia: models for human neurodevelopmental and neurodegenerative disorders. Int J Mol Sci 21:4859.
44. Kowada R, Kodani A, Ida H, Yamaguchi M, Lee IS, Okada Y, Yoshida H (2021) The function of Scox in glial cells is essential for locomotive ability in Drosophila. Sci Rep 11:21207.

https://doi.org/10.5607/en23027